Journal of Membrane Science 499 (2016) 282–289

Contents lists available at ScienceDirect

Journal of Membrane Science

journal homepage: www.elsevier.com/locate/memsci

Membrane capacity and fouling mechanisms for ultrathin nanomembranes in dead-end filtration

J.D. Winans [a,1], K.J.P. Smith [a,1], T.R. Gaborski [b], J.A. Roussie [c], J.L. McGrath [a,*]

[a] Department of Biomedical Engineering, University of Rochester, Rochester, NY, United States
[b] Department of Biomedical Engineering, Rochester Institute of Technology, Rochester, NY, United States
[c] SiMPore, Henrietta, NY, United States

ARTICLE INFO

Article history:
Received 7 September 2015
Received in revised form
22 October 2015
Accepted 23 October 2015
Available online 27 October 2015

Keywords:
Fouling
Nanomembrane
Ultrafiltration
Capacity
Permeability

ABSTRACT

Ultrathin membrane technologies hold promise for improvements in membrane-based separation, however much remains to be learned about the ability of these membranes to support practical filtration processes. Here we examine the performance of new nanoporous silicon nitride (NPN) membranes in dead-end filtration using different methods for generating transmembrane pressure while varying nanoparticle types, sizes and concentrations. We infer membrane fouling by the amount of filtrate generated after a minute of dead-end filtration and show that each of these parameters has a strong influence on the rate of NPN fouling. Inverted centrifugation, which pulls large particles and aggregates away from the membrane as solvent passes through, increases filtrate volumes compared to forward centrifugation. Fitting filtration results to classic fouling models indicate that particles larger than the pores appear to foul membranes *via* cake formation at all concentrations, while filtration with particles much smaller than pores are impacted by pore obstruction before cake build up. Using direct comparisons in centrifuge devices, we show that NPN membranes have a comparable capacity to process suspensions of small colloids by dead end filtration at similar solvent speeds to thicker polycarbonate track-etched membranes, even with permeabilities more than two orders of magnitude higher.

1. Introduction

Ultrafiltration processes separate large and small solutes by forcing colloidal solutions through a nanoporous membrane sieve and have been part of industrial processes for decades [1]. The performance of an ultrafiltration membrane is often limited by fouling, which can occur either through physical pore interactions with the colloids or from a loss of permeability as colloids back up behind the filter. To minimize fouling, large-scale processes are often configured in a stirred cell or tangential flow filtration (TFF) device that sweeps foulant parallel to the membrane throughout the process. Studies have shown the importance of several parameters in the performance of ultrafiltration including species concentration [2,3], solution temperature [4], feed flow rate [5], stir speed [6], pH [7,8], particulate size [3,9], and membrane pore size [3].

In research laboratories, ultrafiltration is most commonly performed in benchtop centrifuges to concentrate samples, perform buffer exchanges, and separate colloids of significantly different sizes. Examples of samples prepared with benchtop centrifugation include proteins [10,11], nanoparticles [12–14], and pathogens [15–17]. Compared to TFF, dead-end ultrafiltration in a centrifuge is simpler, inexpensive, and less diluting of typical small-volume laboratory samples. Without a tangential component to the flow retained colloids can clog membranes quickly even at the laboratory scale and limit their utility.

As reviewed by Bacchin et al., considerable attention has been given in the literature to the investigation of the critical flux, where the flux in a tangential flow or dead-end filtration system is kept below some value so that the dispersive forces in the system will prevent the solute particles from condensing and depositing onto the membrane. At fluxes above this value a highly impermeable cake forms that dramatically decreases performance [18]. Across a variety of membrane types a transition from blockage models to cake filtration is observed after some time [19,20]. Generally, lower fluxes lead to less severe fouling [21–23], as the ameliorating effects of stirring or tangential flow have less of a concentration buildup against which to work. In the filtration of very small (1–100 nm) particles, Brownian back-diffusion is a significant driver of the dispersion of the local concentration

* Corresponding author.
E-mail address: jmcgrath@bme.rochester.edu (J.L. McGrath).
[1] Co-first-authors.

http://dx.doi.org/10.1016/j.memsci.2015.10.053
0376-7388/

increase at the surface of the membrane [24], especially in the absence of stirring or tangential flow.

Over the last decade, silicon manufacturing techniques have been used to create ultrathin (50 nm thick) nanoporous membranes [25,26]. While the recent development of lift-off methods are enabling ultrathin membrane sheets with areas greater than 100 cm^2 [27], the silicon-based chip remains the most common format for nanomembranes, with small sizes ($\sim$25 mm^2) that are suited to laboratory scale ($\sim$1 mL) filtration [26,28]. We have successfully integrated nanomembrane chips into custom-built centrifuge tubes and used the devices to measure the hydraulic permeability and sieving properties of nanomembranes [26]. These experiments have shown that nanomembranes exhibit a significant and expected increase in hydraulic permeability over conventional materials that are $\sim$10–1000$\times$ thicker [28]. Higher permeability alone is not sufficient to enable a membrane to be practically suited for ultrafiltration if its higher permeability is accompanied by a low *capacity* – a measure of the amount of material that can be processed by a membrane before it becomes useless from the effects of fouling [29]. Achieving high capacity is particularly challenging for nanomembranes because only a fraction of the chip area is permeable or 'active' while the rest is rendered impermeable by the silicon support structure.

In this work, we examine fouling and capacity of NPN membranes created using self-assembling pnc-Si [25] as a template. NPN membranes are more mechanically and chemically robust than pnc-Si while exhibiting similar flow and separation characteristics. Because we are interested in small-volume laboratory separations, we focused on the performance of NPN in a 1.5 mL centrifuge tube. We found that the particle type, size and concentration, and the configuration of the system all impacted the capacity of NPN. Particles larger (100 nm) than the pores (37 nm) clog membranes at concentrations three orders lower than particles much smaller (20 nm) than pores. Using a modified version of classic fouling models that account for the loss of head pressure during a centrifuge process, we analyzed temporal flow to determine the mechanisms of fouling for NPN. We found that both particle sizes eventually clog by cake formation but pore restriction can be seen prior to cake formation in the case of small particles. Finally we compared NPN to polycarbonate track-etched (TE) membranes with the same number of pores under identical operating conditions. We find that NPN membranes have a comparable capacity to TE membranes even with permeabilities more than two orders of magnitude higher, and argue that this is a direct result of their much thinner cross section.

2. Experimental

2.1. Nanomembrane fabrication

Complete details regarding membrane fabrication can be found in a previously published work [26]. In summary, a three layer stack of Si_xN_y, amorphous silicon (a-Si), and silicon dioxide (SiO_2) are deposited onto a 300 μm thick double-side-polished Si wafer which undergoes a rapid thermal anneal in order to crystalize the a-Si and form a pnc-Si film. The SiO_2 layer is removed and reactive ion etching in a Trion Minilok RIE transfers the pores into the Si_xN_y film. The pnc-Si mask is removed with a XeF_2 etch. The active membrane areas and chip edges are defined on the back side of the silicon wafer with standard lithography processes and etched using ethylene diamine pyrocatechol. Membranes are imaged in a transmission electron microscope (TEM) (Fig. 1a) and a pore distribution is calculated using custom image processing software (Fig. 1b).

2.2. Separations

Unless otherwise indicated, all separations were performed by assembling the filters into a custom 'SepCon' housing [26]. All SepCons were prewetted with 10 μL buffer on the top and bottom as a means of ensuring a thorough and continuous wetting of the inside of the pores. They were also prewetted as a means of reducing the possibility of antibodies adhering to a dry Si_xN_y surface and prematurely clogging the pores. Reverse centrifugation was performed by modifying both 1.5 mL conical centrifuge tubes and the SepCon assembly. The centrifuge tubes were filled with $\sim$0.5 mL of polydimethylsiloxane (PDMS). The PDMS served to eliminate 'dead volume' below the lowest point that the SepCon could reach in the centrifuge tube, which was just above the conical section. The SepCons were modified by cutting off the top portion of the reservoir that ordinarily rests on the top rim of the centrifuge tube. Removing the top section of the SepCon allows the remaining piece to slide lower than normally into the centrifuge tube, further reducing 'dead volume'. A Beckman Coulter Microfuge 18 centrifuge fitted with a F241.5P angled rotor was used for all centrifugations. All centrifuge separations in either the forward or reverse orientations were done at 3000 rpm (690*g*) unless otherwise noted. Filtrate volumes were determined by measuring the difference in mass of the conical centrifuge tube. Polycarbonate track etched membranes with pore sizes of 30 nm (PCT00313100) and 50 nm (PCT00513100) were purchased from Sterlitech. These membranes were fixed to the SepCon housing using PDMS. The PDMS fixative obscured a variable amount of the active area of each membrane, so a photo was taken of each of the cured membranes used for separations from which an effective

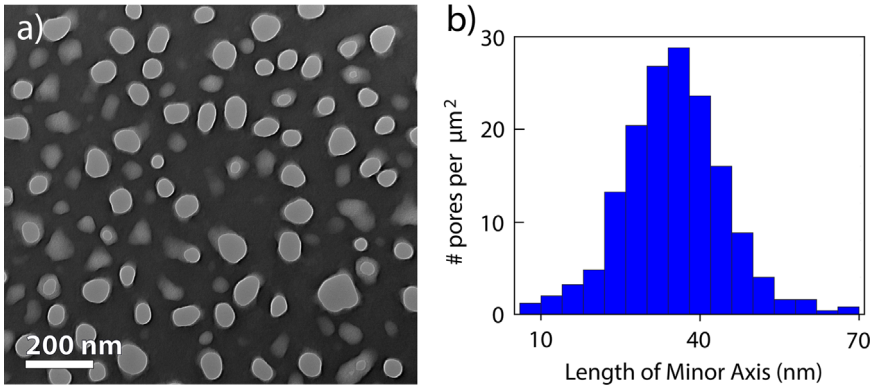

Fig. 1. NPN pore size distribution. a) A TEM image of a NPN nanomembrane. Circles with a rim are pores that span the thickness of the membrane, while gray patches are pits in the surface. b) A pore size histogram generated using image processing software shows that the average minor axis (the restricting axis) is $\sim$37 nm.